Available online at www.sciencedirect.com
SCIENCE DIRECT®
Journal of Non-Crystalline Solids 337 (2004) 191–195
JOURNAL OF NON-CRYSTALLINE SOLIDS
www.elsevier.com/locate/jnoncrysol

Letter to the Editor

# On a qualitative model for the incorporation of fluoride nano-crystals within an oxide glass network in oxy-fluoride glass-ceramics

V.K. Tikhomirov [a], A.B. Seddon [a,*], M. Ferrari [b], M. Montagna [c], L.F. Santos [d], R.M. Almeida [d]

[a] *Novel Photonic Glasses Research Group, Centre for Advanced Materials, University of Nottingham, Nottingham NG7 2RD, UK*
[b] *CNR-IFN, Istituto di Fotonica e Nanotecnologie, 38050 Povo-Trento, Italy*
[c] *INFM, Dipartimento di Fisica, Universita di Trento 38050 Povo-Trento, Italy*
[d] *Departamento de Engenharia de Materiais / INESC-ID, Instituto Superior Técnico, 1049-001 Lisbon, Portugal*

Received 23 December 2003; received in revised form 2 February 2004

**Abstract**

We report on a Raman scattering study of oxy-fluoride glass-ceramics with a typical composition $32SiO_2$:$9AlO_{1.5}$:$31.5CdF_2$:$18.5PbF_2$:$5.5ZnF_2$:$3.5ErF_3$ (in mol%), which indicates a narrow size distribution of β-$PbF_2$ fluoride nano-crystals, typically of $13 \pm 1$ nm, in the silica-based glass network and gives insight on how then nano-crystals are incorporated into the glassy network. The Raman spectra indicate the presence of $Q^0$, $Q^1$ and $Q^2$-like units, which are $SiO_xF_{4-x}$ tetrahedra with zero, one and two bridging oxygens, respectively. The frequency, width and depolarization ratio of Raman bands corresponding to these $Q^n$-like units ($n = 0$, 1, 2) indicate that $Q^0$ units are mostly symmetric $SiO_4$ tetrahedra, $Q^1$ are $SiO_4$ tetrahedra where one F may substitute for O and $Q^2$ are $SiO_4$ tetrahedra where one or two F may substitute for O. We argue that the non-bridging O atoms belonging to $Q^n$ tetrahedra, mostly to $Q^0$ tetrahedra, are located near the interface between the nano-crystalline and glassy phases, allowing an easy accommodation of fluoride nano-crystals with a spherical shape, in the oxide glass network. This was in agreement with the very low-frequency Raman features found between ~4 and 8 $cm^{-1}$, due to acoustic vibrations of the nano-crystals embedded in the glassy matrix.
© 2004 Elsevier B.V. All rights reserved.

*PACS:* 78.66.J; 61.46; 61.14

## 1. Introduction

Rare-earth doped transparent oxy-fluoride glass-ceramics are of great interest for application in telecommunications systems and up-conversion devices (see e.g. recent publications [1,2] and references therein). Although the mechanism for nucleation and growth of rare-earth doped fluoride nano-crystals was suggested to be based on a heat treatment-induced $\alpha \rightarrow \beta$ phase transition of $PbF_2$ [1], the general question concerning how these nano-crystals are structurally accommodated within the glass network has not yet been addressed. And, to our knowledge, the structural incorporation of a nano-crystalline phase into a glassy matrix has not yet been discussed in the literature with respect to other kinds of glass-ceramics.

In this paper, we present and discuss experimental Raman scattering data, which give insights into the size, size distribution and interaction with surroundings of fluoride nano-crystals and also on the mechanism of incorporation of the nano-crystals into the oxide glass-network.

## 2. Experimental

The procedure for preparation of precursor oxy-fluoride glasses with a typical composition $32SiO_2$:

* Corresponding author. Tel.: +44-115 951 3740; fax: +44-115 951 3741.
*E-mail address:* angela.seddon@nottingham.ac.uk (A.B. Seddon).

0022-3093/$ - see front matter © 2004 Elsevier B.V. All rights reserved.
doi:10.1016/j.jnoncrysol.2004.03.114

$9AlO_{1.5}$:31.5$CdF_2$:18.5$PbF_2$:5.5$ZnF_2$:3.5$ErF_3$ (in mol%) and resulting glass-ceramics has been described in [1]. The $AlO_{1.5}/SiO_2$ ratio was varied from sample to sample; this has allowed optimization, at a certain $AlO_{1.5}/SiO_2$ ratio, of the growth of fluoride spherical nano-crystals up to a certain size of about 12 nm diameter [1].

The set-up for measurement of polarized Raman scattering spectra has been described in detail in Ref. [2]. Excitation of scattering was non-resonant, using the 457 nm line of an $Ar^+$ laser at about 100 mW, where the $Er^{3+}$ dopant and oxy-fluoride host do not absorb the exciting light. The spectra were measured in a 90° geometry and deconvolution of the obtained data was carried out using Origin 7.0 software.

## 3. Results

Polarized Raman spectra for the above glass and resulting glass-ceramics have been shown elsewhere [2]. Assignment of the observed scattering bands was also carried out in [2].

Fig. 1 shows the Stokes and anti-Stokes ultra-low frequency regions of the Raman spectra in the vertical–vertical (VV) polarized configuration (thin solid line). The Stokes and anti-Stokes parts are symmetric, since, at room temperature $T$, $h\omega/2\pi \ll kT$ for this low-frequency ($\omega$) range. The background, represented by the dotted line, was subtracted and the resulting curve was fitted with two Lorentzian peaks shown by dashed lines, for the Stokes and anti-Stokes parts. The resulting fit is depicted by a thick solid line. Table 1 summarizes the parameters of the fit.

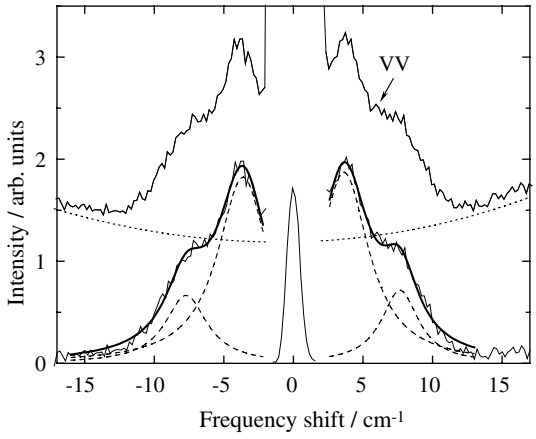


Fig. 1. Low-frequency Stokes and anti-Stokes Raman scattering spectra of the glass-ceramics corresponding to the base glass $32SiO_2$:$9AlO_{1.5}$:31.5$CdF_2$:18.5$PbF_2$:5.5$ZnF_2$:3.5$ErF_3$, in the polarized VV configuration, as measured and after subtraction of background (noisy solid curves). The background is depicted by the dotted line. Dashed lines represent two Lorentzian crystalline-like peaks and the thick, smooth solid line is the resulting fits. The peak at 0 $cm^{-1}$ corresponds to the laser line, attenuated 1000 times.

Table 1
Parameters of the Lorentzian fit of the low-frequency VV (see Fig. 1) and HV-polarized Raman spectra of glass-ceramics corresponding to the base glass, averaged over Stokes and anti-Stokes parts

| | $\omega$ ($cm^{-1}$) | FWHM ($cm^{-1}$) | I (arb.u.) |
|---|---|---|---|
| $l = 2$ | | | |
| VV | 3.6 | 4.3 | 12.4 |
| HV | 3.6 | 3.8 | 8.6 |
| $l = 0$ | | | |
| VV | 7.7 | 3.6 | 3.9 |
| HV | 8.9 | 3.1 | 0.7 |

$\omega$ stands for peak frequency, FWHM for full width at half maximum and I for integrated peak intensity. $l = 0$ and 2 stand for symmetric and quadrupolar vibrations, respectively.

Fig. 2 shows the high frequency regions of the polarized Raman spectra, which correspond to $Q^n$-like vibrations in the silicate glass network (see e.g. review [3] on Raman scattering in silicate glasses). The spectrum of the base glass $32SiO_2$:$9AlO_{1.5}$:31.5$CdF_2$:18.5$PbF_2$:5.5$ZnF_2$:3.5$ErF_3$ (in mol%) is shown in Fig. 2(a); that of the glass enriched in $AlO_{1.5}$ is shown in Fig. 2(b) and that of the glass enriched in $SiO_2$ (compared to the base glass) is shown in Fig. 2(c).

## 4. Discussion

The deconvolution shown in Fig. 1 yielded the parameters listed in Table 1. These include frequencies well below the Boson peak, which occurs at about 70 $cm^{-1}$ [2]. These bands may be attributed to the accoustic vibrations of nano-particles embedded in the glassy network [4–6]. Two types of vibrations are possible: spheroidal and torsional. They are labelled, as in the case of a free homogeneous elastic spherical particle, according to the symmetry group of the sphere, by the quantum numbers $l$ and $m$. Only the spherical modes with $l = 0$ and 2 are Raman active, which are the surface symmetric and quadrupolar modes, respectively [6]. The $l = 2$ mode is active both in VV and HV polarizations, while $l = 0$ mode is active only in VV polarization, in agreement with the experimental data given in Table 1. The actual spherical nano-particles in our case are β-$PbF_2$ nano-crystals doped with $Er^{3+}$ ions [1]. The frequencies for $l = 0$ and 2 modes are given by Eq. (1):

$$\omega_j = \frac{S_j v_j}{dc}, \tag{1}$$

where $j = 0$ or 2; $\omega_0$ and $\omega_2$ are the frequencies of symmetric and quadrupolar vibrations, respectively, $S_0$ and $S_2$ are constants close to 1 and defined by the ratio of the longitudinal $v_0 = v_L = 3470$ m/s and transversal $v_2 = v_T = 1730$ m/s sound velocities in β-$PbF_2$ [7], $d$ is

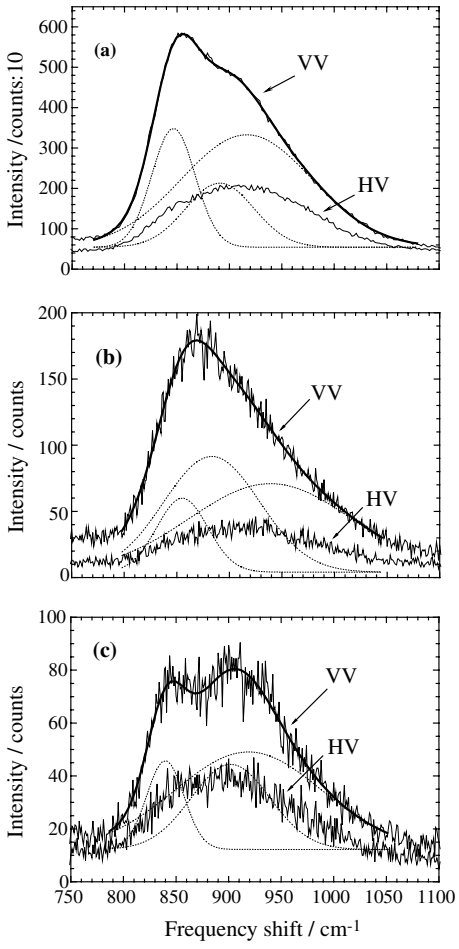


Fig. 2. Raman scattering spectrum of (a) the base glass, $32SiO_2$:$9AlO_{1.5}$:$31.5CdF_2$:$18.5PbF_2$:$5.5ZnF_2$:$3.5ErF_3$; (b) $AlO_{1.5}$-enriched glass, $26SiO_2$:$15AlO_{1.5}$:$31.5CdF_2$:$18.5PbF_2$:$5.5ZnF_2$:$3.5ErF_3$; (c) $SiO_2$-enriched glass, $38SiO_2$:$3AlO_{1.5}$:$31.5CdF_2$:$18.5PbF_2$:$5.5ZnF_2$:$3.5ErF_3$ in the polarized (VV, upper thin solid line) and depolarized (HV, lower thin solid line) configurations in the region, which corresponds to $Q^{(n)}$-type vibrations in the silicate glass network. Deconvolution of the VV spectrum in the three components $Q^0$ (at about 850 $cm^{-1}$), $Q^1$ (at about 890 $cm^{-1}$) and $Q^2$ (at about 920 $cm^{-1}$) is represented by three Gaussian peaks (dotted lines), respectively and the thick solid line is the resulting fit.

the diameter of the nano-particles and $c$ is the light velocity. After [5], $S_0 = 0.87$ and $S_2 = 0.84$, i.e. $S_0 v_L / S_2 v_T = 2.07$, in good agreement with the experimentally observed ratio $\omega_0/\omega_2 = 2.1$. The mean diameter of nano-particles, calculated from Eq. (1) is then 13 nm, only slightly larger than the value 12 nm obtained from X-ray diffraction and transmission electron microscopy (TEM) measurements [1]. The difference is accounted for by the experimental error.

The band corresponding to the $l = 0$ mode at 7.7 $cm^{-1}$ has a relative linewidth $\mathrm{FWHM}/\omega_0 = 0.5$ (Table 1), where FWHM stands for full width at half maximum. There are two sources for this linewidth broadening: homogeneous and inhomogeneous. While the former one is due to phonon interaction of the nano-particles with the surrounding glass network [5], the latter one is related to varying particle size, as can be seen from the Eq. (1). The homogeneous broadening can be estimated based on values for density and elastic constants of nano-particles and surrounding glass network [5]. The result of the estimate is that the homogeneous linewidth at $\mathrm{FWHM}/\omega_0 = 0.7$ is larger than the observed one at $\mathrm{FWHM}/\omega_0 = 0.5$ (Table 1); therefore, the experimental linewidth can be accounted for without the contribution of inhomogeneous broadening, apparently not important compared to the total linewidth. We conclude that the size distribution of the spherical nano-particles is narrow (within $\pm 1$ nm), in agreement with direct measurements by (TEM) [1]. On the other hand, as the estimated value for the linewidth based on homogeneous broadening is larger than the experimental value, we conclude that phonon interaction of nano-particles with the surrounding glass network is weaker than the interaction calculated based on the density and elastic constants of the crystalline nano-particles and surrounding glass. Therefore, the nano-particles appear not to be well bonded to the surrounding glass matrix, e.g. by means of covalent bonding. Further support for this conclusion is found by analyzing the high frequency part of the Raman spectrum, related to $Q^n$-like units (Fig. 2), as discussed below.

The spectral deconvolution shown in Fig. 2 indicates that $Q^n$-type $(n = 0, 1, 2)$ units are present with a ratio between corresponding areas of $Q^0$:$Q^1$:$Q^2 = 21$:18:61 (in percentage units) for the base glass (Fig. 2(a)), $Q^0$:$Q^1$:$Q^2 = 13$:49:38, for the glass enriched in $AlO_{1.5}$ compared to the base glass (Fig. 2(b)), and $Q^0$:$Q^1$:$Q^2 =$ 14:27:59, for the glass enriched in $SiO_2$ compared to the base glass (Fig. 2(c)). These $Q^n$ units are schematically depicted in Fig. 3. The Raman spectra of the corresponding glass-ceramics were the same as for the precursor glass, in the region corresponding to Q-type vibrations [2]. The glass-ceramics corresponding to the base glass (Fig. 2(a)), with the composition $32SiO_2$: $9AlO_{1.5}$:$31.5CdF_2$:$18.5PbF_2$:$5.5ZnF_2$:$3.5ErF_3$ (in mol%), was shown by means of TEM to contain *spherical* β-$PbF_2$ nano-particles [1]. The nano-particles, however, were irregular and dendritic-shaped in glass-ceramics corresponding to $AlO_{1.5}$ (Fig. 2(b))- and $SiO_2$ (Fig. 2(c))-enriched compositions; these latter glass-ceramics were also more prone to crystallization than the one originating from the base glass. This glass-ceramics derived from the base glass contained the largest proportion of $Q^0$ units, which appeared to promote the formation of spherically shaped nano-particles. We suggest that the $Q^0$ units are located preferentially at the interface between crystalline and glassy phases, thus hindering further growth of fluoride nano-particles above 13 nm in diameter and simultaneously releasing stresses, which are likely to appear with the formation of nano-particles

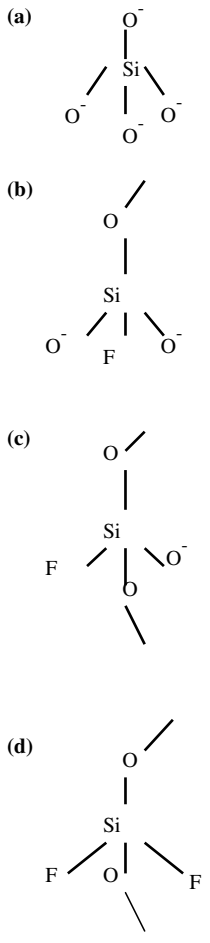


Fig. 3. Schematic picture of: (a) $Q^0$, (b) $Q^1$ and (c), (d) $Q^2$ tetrahedra, in the oxy-fluoride glass-ceramic $32SiO_2{:}9AlO_{1.5}{:}31.5CdF_2{:}18.5PbF_2{:}5.5ZnF_2{:}3.5ErF_3$.

of lower molar volume ($\sim 3.16\times10^{-5}$ m$^3$/mol) within a glass matrix of larger molar volume ($3.6\times10^{-5}$ m$^3$/mol). Since all oxygen atoms belonging to $Q^0$ are non-bridging, the chemical bonding between the crystalline nanoparticles and the surrounding glass will be more ionic (or less covalent) and therefore weaker, in agreement with the conclusion drawn above, based on the analysis of low-frequency Raman scattering (Fig. 1 and Table 1).

The frequency of the Raman band at about 850 cm$^{-1}$, corresponding to $Q^0$-like units in Fig. 2(a)–(c), agrees well with the frequency of $Q^0$ units in silicate glasses without admixture of fluorides (at 850 cm$^{-1}$) [3]. Therefore we suggest that $Q^0$-like units in the case of oxy-fluoride glass-ceramics are the same as in silicate glasses, i.e. $SiO_4$ tetrahedra without bridging oxygens. The relatively small width of the $Q^0$ band in Fig. 2(a)–(c) indicates that such tetrahedra, as depicted in Fig. 3(a), do not differ much from each other. The frequency at about 890 cm$^{-1}$ corresponding to $Q^1$-like units in Fig. 2(a)–(c), is lower than the frequency of $Q^1$ units in silicate glasses (at 900 cm$^{-1}$) [3]. This can be explained taking into account that one F atom may substitute for O in some of the $SiO_4$ tetrahedra (Fig. 3(b)) resulting in the relatively small shift to lower frequency of $Q^1$ vibration (breathing mode $A_1$ [3]). The substitution F for some of O will also result in broadening the vibrational band, in agreement with the data of Fig. 2(a)–(c), where the linewidth of $Q^1$ is substantially larger that the linewidth of $Q^0$. The frequency at about 920 cm$^{-1}$ corresponding to $Q^2$-like units in Fig. 2(a)–(c), differs even further from the frequency of $Q^2$ units in silicate glasses (at 950–1000 cm$^{-1}$) [3]. Therefore, we suggest that one or even two F may substitute for O in some of the $SiO_4$ tetrahedra (Fig. 3(c) and (d)) resulting in even larger shifts to lower frequency of $Q^2$ vibration, as observed in Fig. 2(a)–(c). Such substitution results in further broadening of the $Q^2$ band, as observed in these figures.

A qualitative comparison of the data for polarized (VV) and depolarized (HV) configurations in Fig. 2, indicates that the $Q^0$ band is well polarized, while the $Q^1$ band is less polarized and $Q^2$ is further less polarized. (It is difficult to present quantitative values for the depolarization ratio, because the HV spectra were featureless). These data confirm the structure of $Q^n$-like units suggested in Fig. 3, where the $Q^0$-like unit is symmetric, the $Q^1$-like is less symmetric due to presence of F and the $Q^2$-like is further less symmetric due to presence of one or two F species. Since the vibrations corresponding to $Q^n$ tetrahedral, in the frequency range presented in Fig. 2, are the symmetric breathing modes $A_1$(see e.g. [3]), then the progressing depolarization of $Q^n$-bands in Fig. 2 should be due to a lowering symmetry of $Q^n$-like units from $Q^0$ to $Q^1$ and further to $Q^2$, in agreement with Fig. 3.

## 5. Conclusion

Alumino-silicate oxy-fluoride glass-ceramics were studied by polarized Raman spectroscopy. The low-frequency spectra indicate the presence of a narrow distribution of the fluoride nano-crystals with an average size of $\sim$13 nm. The high frequency portion of the spectra indicates the presence of $Q^n$-like units of the $Q^0$, $Q^1$ and $Q^2$ types, with $Q^2$ being usually predominant. The $Q^0$ units appear to be preferentially located near the interface between the fluoride nano-crystals and the oxide glass network. Thus, the covalent bonding is only of minor importance in the structure linkage between nano-crystalline and glassy phases, dominated by weaker ionic bonds.

## Acknowledgements

V.K.T. gratefully acknowledge the co-authors from Trento and Lisbon for hospitality during the visits.

## References

[1] V.K. Tikhomirov, D. Furniss, A.B. Seddon, I.M. Reaney, M. Beggiora, M. Ferrari, M. Montagna, R. Rolli, Appl. Phys. Lett. 81 (2002) 1937.
[2] V.K. Tikhomirov, A.B. Seddon, M. Ferrari, M. Montagna, L.F. Santos, R.M. Almeida, Europhys. Lett. 64 (2003) 529.
[3] P. McMillan, Am. Mineral. 69 (1984) 622.
[4] E. Duval, A. Boukenter, B. Champagnon, Phys. Rev. Lett. 56 (1986) 2052.
[5] M. Montagna, R. Dusi, Phys. Rev. B 52 (1995) 10080.
[6] E. Duval, Phys. Rev. B 46 (1992) 5795.
[7] M.O. Manasreh, D.O. Pederson, Phys. Rev. B 30 (1984) 3482.